Combustion and Flame 251 (2023) 112737

Contents lists available at ScienceDirect

Combustion and Flame

journal homepage: www.elsevier.com/locate/combustflame

Flame propagation of combustible dusts: A Mallard-Le Chatelier inspired model

M. Portarapillo[a,*], R. Sanchirico[b], G. Luciani[a], A. Di Benedetto[a]

[a] Dipartimento di Ingegneria Chimica, dei Materiali e della Produzione Industriale, Università degli Studi di Napoli Federico II, Piazzale V. Tecchio 80, 80125 Napoli, IT, Italy
[b] Istituto di Scienze e Tecnologie per l'Energia e la Mobilità Sostenibili (STEMS), Consiglio Nazionale delle Ricerche (CNR), Piazzale V. Tecchio 80, 80125, Napoli, IT, Italy

ARTICLE INFO

Article history:
Received 12 October 2022
Revised 9 March 2023
Accepted 10 March 2023
Available online 24 March 2023

Keywords:
Flame propagation
Dust burning velocity
Mallard-Le Chatelier theory
Cornstarch
Lycopodium

ABSTRACT

In this work, a three-layers Mallard-Le Chatelier inspired theoretical model is developed to fully characterise the steps occurring during the flame propagation of combustible dusts/air. The model is based on the hypothesis that the dust flame propagation follows a homogeneous path: the dust-air mixture is pre-heated up to the volatile point (*VP*), at which production of volatiles occurs, thanks to the back-diffusion of heat from the combustion zone of the flame to the colder zones. The volatiles produced are then heated up to the ignition temperature and enter in the combustion zone. The flame burning velocity is the results of the coupling between heating rate, pyrolysis and/or evaporation/sublimation rate and volatiles combustion rate. The rate of formation of volatiles was measured by means of *TG/DSC* analysis. The laminar burning velocity of gases was computed by simulating the gas flame propagation in a tube starting from the measured gas compositions (by literature data or *FTIR* analysis).

1. Introduction

The severity of a dust explosion strongly depends on the mode of flame propagation. Dust clouds with different thermal characteristics and particle size distributions would form entirely different flame structures. Two types of flames can be distinguished. The first, the Nusselt type, is controlled by the diffusion of oxygen to the surface of individual solid particles, where the heterogeneous chemical reaction takes place (Path A in Fig. 1). In the second type, the volatile flame, the rate of gasification, pyrolysis, or devolatilization is the controlling process and the chemical reaction takes place mainly in the homogeneous gas phase (Path B in Fig. 1) [1,2]. To decide which is the main flame propagation path, there are two key parameters, namely the ability of the condensed fuel to volatilise and form a premixed fuel-oxidant gas mixture prior to combustion and the stability of the premixed fuel-oxidant vapour mixtures at temperatures close to the boiling point of the fuel [3]. More specifically, in the case of organic powders, the production of flammable volatiles can take place through physical phenomena of fusion/evaporation and/or sublimation as in the case of niacin, or through pyrolysis processes [4,36].

In this work, the focus will be on Path B. In this case, during the flame propagation, most dusts have to be heated up to reach the temperature at which flammable volatiles are produced, *VP* [5]. In this heating phase, two main paths of volatile production processes may occur: physical transformations (sublimation and/or melting-boiling) and/or chemical reactions (i.e., pyrolysis) [6]. When volatiles are produced, combustion of the gas products starts. All these steps are coupled and are strongly affected by the particle size. Di Benedetto et al. (2010) studied this effect on the dust reactivity developing a model that considers all the steps above mentioned. Varying the dust size, they identified different regimes depending on the values of the characteristic time of each step, as function of dimensionless numbers [7]. Several studies on the flame propagation for the dusts, in particular for the measurement of the laminar burning velocity, have been carried out mainly by using tube method, however the knowledge on the fundamental mechanisms of flame propagation in dust-air mixtures is still lacking ([8–10]).

The experimental measurement of the dust flame propagation velocity is strongly dependent on the turbulence generated inside the test vessel. To generate dust flame propagation the dust particles must be dispersed and suspended in air generating a cloud. Dispersion and suspension of dust particles are generated thanks to some degree of turbulence which is then always present in the dust cloud before ignition. In the test devices, turbulence structures and turbulence kinetic energy level may vary from one apparatus to another, depending on the dispersion method and the

* Corresponding author.
E-mail address: maria.portarapillo@unina.it (M. Portarapillo).

https://doi.org/10.1016/j.combustflame.2023.112737

Nomenclature

A	Cross sectional area (m^2)
C_{dust}	Nominal dust concentration present inside the test reactor (kg/m^3)
Cp_{dust}	Dust heat capacity (J/(kg·K))
$Cp_{dust+air}$	Dust heat capacity mixed with air in the dust dispersion (J/(kg·K))
$Cp_{gas,II}$	Heat capacity of gaseous species produced through devolatilization (J/(kg·K))
f_{dust}	Mass fractions of dust in the dust dispersion (-)
f_{air}	Mass fractions of air in the dust dispersion (-)
$\dot{m}_{dev}$	Mass rate of gaseous species produced through devolatilization (kg/s)
$\dot{m}_{dust}$	Mass rate of dust (kg/s)
P_{amb}	Ambient pressure, reference status (1 bar)
$P_{unburned}$	Initial pressure of dust at which ignition occurs (bar)
S_{dust}	Dust burning velocity (m/s)
$S_{dust,\ T,P}$	Dust burning velocity at initial temperature and pressure different from the reference values (25°C and 1 bar) (m/s)
S_l	Gas laminar burning rate (m/s)
T_{ad}	Adiabatic temperature (K)
T_{amb}	Ambient temperature, reference status (298 K)
T_{ign}	Ignition temperature (K)
$T_{unburned}$	Temperature of unburned dust at which ignition occurs (K)
VP	Volatile point (K)
Greek	
B	Empirical constant (-)
δ_{III}	Reaction zone thickness (m)
δ_{II}	Gas pre-heating zone thickness (m)
ΔH_{dev}	Heat of devolatilization (J/kg)
λ_{III}	Thermal conductivity of burned gases (*W/(m·K)*)
λ_{II}	Thermal conductivity of unburned gases (*W/(m·K)*)
ρ_{dev}	Density of gaseous species produced through devolatilization (kg/m^3)
ρ_{dust}	Dust density (kg/m^3)
$\rho_{dust+air}$	Dust density mixed with air in the dust dispersion (kg/m^3)

vessel geometry. Therefore, the measured values of the dust laminar burning velocity may vary from one researcher to another.

By way of example, measurements of the laminar burning velocity of cornstarch-air mixtures are shown in Fig. 2. Proust and Veyssière (1988) observed and evaluated the flame propagation of cornstarch-air mixtures (mean diameter 20 µm, concentration 100–220 g/m^3) in a 3 m long tube where the dust dispersion was realized though the elutriation above a fluidized bed [11]. Proust (1993) assessed S_l within a 1.5 m long tube where the dust dispersion was obtained though the elutriation above a fluidized bed for starch dust-air mixtures, lycopodium-air mixtures and sulphur flower-air mixtures (mean particle diameter 25–45 µm, concentration 100–300 g/m^3) through the tube and direct methods [12]. Nagy and Verakis (1983) derived laminar burning velocities and the deflagration index for clouds at 500 g/m^3 concentration of several dusts through experimental dust explosion data from the elongated 1.2 litre Hartmann bomb [13]. Mazurkiewicz et al. (1993) measured the laminar burning velocity of cornstarch-air flames (mean particle diameter 15 µm, concentration 500 g/m^3) in a vertical 50 × 50 mm square tube, 1 m long, where the suspension was generated through elutriation of dust particles above a fluidized bed [14].

van Wingerden and Stavseng (1996) measured the laminar burning velocity of cornstarch-air and maize starch-air flames (mean particle diameter <100 µm, concentration 80–200 g/m^3 and 45–300 g/m^3, respectively) in an 1.6 m long vertical tube made of transparent polycarbonate where the dust was supplied continuously into the top of the tube from a horizontally vibrating sieve and a vibratory dust feeder [15]. The burning velocity in laminar flows was studied in a vertical cylindrical tube of 2 m in length and 300 mm in diameter where dust was layered on a porous filter plate and elutriated in a fluidized bed at the beginning of each experiment by Krause and Kasch (1994) [16]. In Fig. 2, it is possible to note the large deviation of the measured values especially at low dust concentration.

To support the experimental measurements as well as to have an order of magnitude of the laminar burning velocity when experimental data are absent, it is then very useful to have a modelling tool able to calculate the value of the laminar burning velocity of the dust/air mixtures.

Some thermal theories of laminar flame propagation for combustible dusts are already developed and can be found in the literature. The advantage of thermal theories of flame propagation is their simplicity. The thermal theory of Cassel et al. (1948) is based on a modification of Mallard-Le Chatelier model for laminar flame propagation, including radiation effect. This radiation model of Cassel and his colleagues was never formally tested against experimental measurements. Moreover, To calculate a burning velocity for a dust flame using the radiation-modified Mallard-Le Chatelier model, one must estimate the ignition temperature, the burnout time, and the emissivity of the flame. Of these parameters, the ignition temperature of the combustible dust is the one that carries with it the most uncertainty [17]. To overcome this limitation, Ogle et al. derived an expression for the burning velocity of a dust flame without invoking an ignition temperature. The model is based on a mixture formulation for the two-phase mixture with constant properties. This model does not require the introduction of an ignition temperature, but it requires the specification of the flame temperature [18]. Both these simple theories do not seem capable of accurate prediction of the burning velocity. An improvement on the thermal theory was due to Ballal and his colleagues in which they combine a time scale analysis to an energy balance on the flame. Ballal model strength lies in the simplicity of its formulation and its reliance on single particle combustion models. Its primary weakness is that it requires the same input parameters required by the thermal theories, plus many more. Perhaps its greatest weakness is that it requires the specification of an ignition temperature. Thus, while many of the input parameters can be calculated a priori as physical properties, some, like ignition temperature, require empirical measurement [19]. Generally, in the available models, there are numerous parameters required as inputs to the model that are often complex to evaluate, and there is a limited evaluation of chemical and physical features that may influence the propagative phenomenon.

In this work we present a theoretical flame propagation model for combustible dusts to support experimental evaluations and/or to make preliminary considerations of the intrinsic laminar burning velocity as a function of characteristics thermal, chemical and physical features. The model is developed and tested by the aid of thermal and chemico-physical characterization for all the combustible dusts to assess key parameters influencing the flame propagation.

2. Model development

In the dust flame thickness (Fig. 3), we identified three zones: zone I, zone II and zone III. In the zone I, the dust is pre-heated up to the volatile point (*VP*) at which devolatilization occurs. This

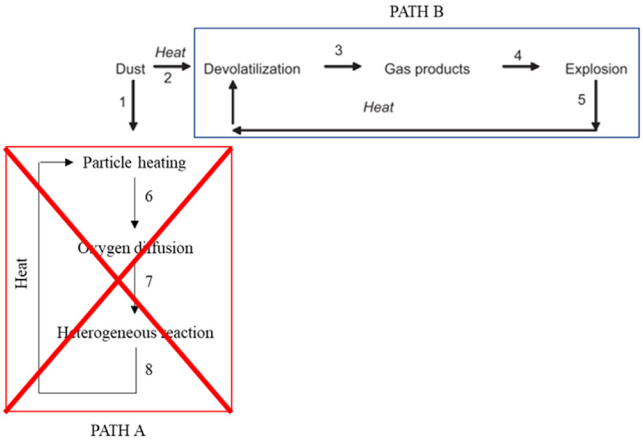

Fig. 1. Schematic representation of the paths occurring during dust explosion. Path A has been deleted to clarify the main focus of the present work.

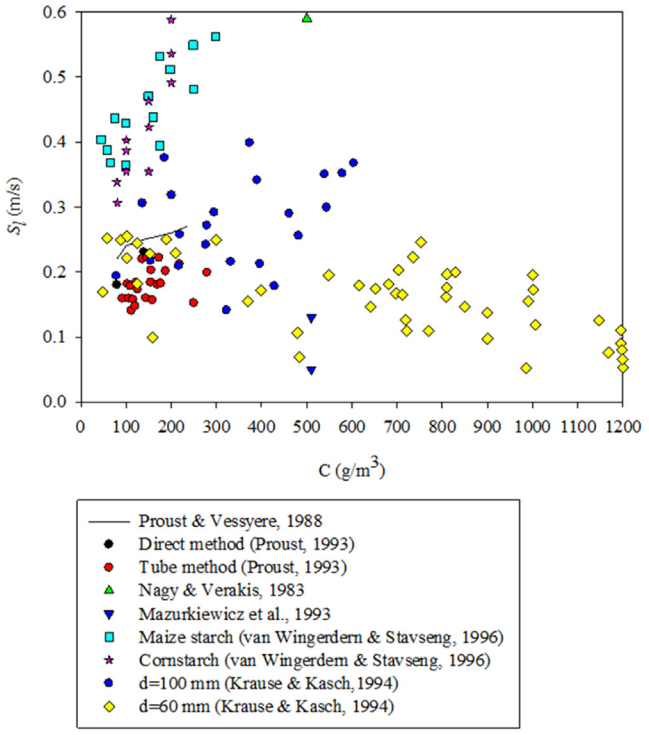

Fig. 2. Literature data about laminar burning velocity of cornstarch as a function of dust concentration ([11–16]).

is the only layer relative to the solid phase. In the zone II, the produced gases are pre-heated up to the ignition temperature (T_{ign}). The zone III is the reaction zone where temperature reaches the adiabatic temperature (T_{ad}).

As stated by Mallard and Le Chatelier (1883) [20], the heat diffusing from zone III to zone II and zone I in Fig. 3 is equal to that necessary to raise the dust to the volatile point (the boundary between zones I and II), sustain the devolatilization and to heat up the unburned gases to the ignition temperature (the boundary between zones II and III). If it is assumed that the slope of the temperature curve is linear, the heat back diffusing can be evaluated by the following expression:

$$\frac{\left(T_{ad}-T_{ign}\right)}{\delta_{III}} \tag{1}$$

Where δ_{III} (m) is the thickness of the reaction zone.

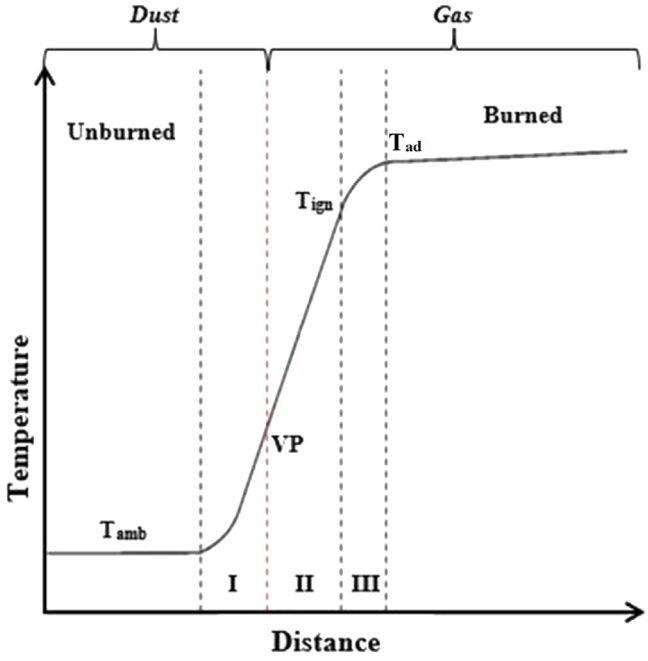

Fig. 3. Proposed thermal profile of dusts and dust mixtures flames.

Eqs. (2), (3) and (4) represent the energy balances and the condition of equality of heat quantities in a series of layers:

$$\lambda_{II}\frac{\left(T_{ign}-VP\right)}{\delta_{II}}A = \dot{m}_{dust}\left(Cp_{dust+air}(VP-25)+\Delta H_{dev}\right) \tag{2}$$

$$\lambda_{III}\frac{\left(T_{ad}-T_{ign}\right)}{\delta_{III}}A = \dot{m}_{dev}\,Cp_{gas,II}\left(T_{ign}-VP\right) \tag{3}$$

$$\lambda_{III}\frac{\left(T_{ad}-T_{ign}\right)}{\delta_{III}}A = \lambda_{II}\frac{\left(T_{ign}-VP\right)}{\delta_{II}}A \tag{4}$$

Where λ_{II} and λ_{III} ($W/m°C$) are the thermal conductivity of gases in the zone II and III, δ_{II} (m) is the thickness of the II zone, $Cp_{gas,II}$ (J/kg°C) is the specific heat of the unburnt gases, $\dot{m}_{dev}$ (kg/s) is the mass rate of the unburnt gas mixture produced by devolatilization into the combustion wave, $\dot{m}_{dust}$ (kg/s) is the mass rate of the combustible dust, $Cp_{dust+air}$ (J/kg°C) is the specific heat of the combustible dust mixed with air, ΔH_{dev} (J/kg) is the devolatilization heat and A (m^2) is the cross-sectional area.

Mass balance equations are the following:

$$\dot{m}_{dev} = \rho_{dev}uA = \rho_{dev}S_lA \tag{5}$$

$$\dot{m}_{dust} = \rho_{dust\ +\ air}S_{dust}A \tag{6}$$

where ρ_{dev} (kg/m^3) is the density of unburnt gases, S_l (m/s) is the laminar burning velocity of the gaseous mixture with air, S_{dust} (m/s) is the laminar burning velocity of the combustible dust and $\rho_{dust+air}$ (kg/m^3) is the particles density mixed with air.

$Cp_{dust+air}$ and $\rho_{dust+air}$ can be calculated as the weighted average of the properties of the dust and the air:

$$\rho_{dust+air} = f_{dust}\rho_{dust} + f_{air}\rho_{air} \tag{7}$$

$$Cp_{dust+air} = f_{dust}Cp_{dust} + f_{air}Cp_{air} \tag{8}$$

Where f_{dust} (-) and f_{air} (-) are mass fractions of dust and air respectively and can be calculated as

$$f_{dust} = \frac{C_{dust}}{\rho_{dust}} = 1 - f_{air} \tag{9}$$

Where C_{dust} (kg/m^3) is the nominal dust concentration present inside the test reactor, Cp_{dust} (J/kg°C) is the specific heat of the combustible dust and ρ_{dust} (kg/m^3) is the particles density.

By rearranging all the equations, the following expression can be obtained:

$$S_{dust} = \frac{\rho_{dev} S_l Cp_{gas,II}\left(T_{ign} - VP\right)}{\rho_{dust+air}\left(Cp_{dust+air}(VP - 25) + \Delta H_{dev}\right)} \quad (10)$$

The theoretical model was applied by way of example on cornstarch and lycopodium. To calculate the dust burning velocity (S_{dust}), several parameters have to be estimated.

3. Limitations of the model

The mathematical model here developed is characterized by both potential and limitations.

In the current model version, there are some limitations such as:

- Radiative heat transfer is not considered in the model, whereas it is well known that it plays a significant role in the flame propagation.
- The composition as well as the amount of the produced gases depends on the dust concentration. In the current calculations, no variation of gaseous composition was considered.
- The effect of heating rate is of crucial importance to characterize the generated gases. In these calculations, this effect was not investigated, and the heating rate used is not that typical of a dust explosion. It is worth noting that the heating rate strongly influences the composition of the generated gases and consequently the autoignition temperature T_{ign} and the adiabatic temperature T_{ad}. However, this issue is already present in the VP assessment procedure, although the procedure is that contained in the relevant standard [21].
- The model cannot be applied to non-volatile solid fuel suspensions since in that case several phenomena strongly related to the heterogeneous path of flame propagation must be taken into account as summarize in a recent work [3].
- The model is applicable for dusts characterized by a Biot number value Bi<<1 [7,22]. In this conditions, the internal heat transfer rate is much faster than the external heat transfer rate and the thermal conversion process is dominated by the external heat transfer supply. On the contrary, the model considers the external heat transport, the devolatilization of the dust and the combustion of the gases produced. One of these steps may be limiting depending on the dust considered. For this reason, the model can be used for powders characterised by any value of Damköhler number and Pc number. Notably, Damköhler number compares the characteristic time of external heat transport with that of the devolatilization, while the Pc number compares the characteristic time of the devolatilization with the characteristic time of volatile combustion.

4. Model validation

4.1. Materials and methods

These parameters as well as the measurement/calculation procedures are listed in Table 1, together with a summary of the procedures used for their estimation, reported in detail below.

First, the dust properties were found in the literature data or, in the case of density, estimated by liquid pycnometry as already used for the characterisation of powders used in the food industry [24].

The flash point is the lowest temperature at which a liquid generates enough vapours to form a mixture with air (or another oxidative agent, such as pure oxygen) at lower flammable limit (*LFL*). For dusts that are characterized by a homogeneous combustion, a specular parameter was proposed [5]. The Volatile Point (*VP*) represents the temperature at which pure dusts, dust mixtures and hybrid mixtures are able to produce volatiles which form, in contact with an oxidizing medium, a flammable vapor mixture at *LFL*. Volatile Point was measured by using the same apparatus used for Flash Point (*FP*). The device is a closed cup instrument that allows the measurement of *FP*/*VP* for liquid/solid samples following different international standards over the range ambient to 300°C [21]. Notably, *VP* is the first temperature at which produced gases are produced at a flammable concentration with air but increasing temperature the composition as well as the amount of gases may vary.

The heat of devolatilization (ΔH_{dev}) was assessed by using a *TG/DSC* TA Instrument Q600SDT, opportunely calibrated. It is worth noting that this parameter, as well as in *VP*, contains the effect of the dust size. Tests were performed in open alumina pan and in N_2 atmosphere, where 10 mg sample was placed in the crucible and was heated up with heating rate β = 20.0°C/min, to improve *DSC* sensitivity. Moreover, volatile matter was determined by measuring the weight loss when heated up to 1000°C in the same operating conditions [25].

Starting from each volatiles composition, we performed the simulation of the flame propagation of volatiles (S_l) by means of the software CHEMKIN and evaluated the laminar burning velocity [26]. Particularly, we modelled the flame as steady, isobaric, quasi-one-dimensional flame, through the Premixed Laminar Flame-speed Calculation. GRI-Mech 3.0 was involved as optimized mechanism of gas-phase reactions opportunely designed to model natural gas combustion in the case of cornstarch [27]. For lycopodium, since butane was found as the main component of the gaseous phase, the reduced mechanism for flames of n-butane developed by Kumaran et al. (2021) was implemented in CHEMKIN solver [28].

Moreover, other properties, such as the volatiles density ρ_{dev} and heat capacity $Cp_{gas,II}$ were calculated as the weight average values. As regards the parameters which values are variable (i.e., functions of dust concentration), their calculations were performed once set the composition of gases produced by literature data and/or measurements. In the case of lycopodium, the experiment for *VP* evaluation, typically carried out in the flash point apparatus, was replicated in the *TG/DSC* equipment in open cup conditions to assess the gaseous species present at *VP*. 10 mg sample were heated up to *VP* (210°C) (heating rate 20°C/min) in airflow and the produced gases were continuously analysed by means of an *FTIR* gas through *TGA/FTIR* interface linked by transfer line to *TGA* furnace. The cell and transfer line of the *TGA/FTIR* interface were heated and kept at 220°C. In this way, product gases from samples degradation could not condense. Surprisingly, analysing the *FTIR* spectra at the maximum of the Gram-Schmidt diagram, butane can be considered as the main gaseous product at *VP*. The HR Nicolet TGA Vapor Phase library of OMNIC software has been used to recognise the produced gases [29].

4.2. Results and model validation

In Figs. 4 and 5, the trends of S_{dust} as a function of *VP* parametric in S_l and ΔH_{dev} are reported. By increasing S_l, S_{dust} increases because the gas produced by devolatilization of the dust are characterized by a higher flame propagation velocity. In this condition, the phenomena involved in the I phase (the devolatilization) control the flame propagation. Conversely, by decreasing ΔH_{dev}, S_{dust} increases because the dust devolatilization subtracts a lower amount of energy from the flame and the remaining energy can be used for the dust and gases pre-heating. In this condition, the devolatilization is a fast step and it does not control the flame prop-

Table 1
Theoretical model parameters and procedures for their measurement and/or calculation.

Parameters	Procedure
$\rho_{dust+air}$ and $Cp_{dust+air}$	Bulk density and heat capacity of the dust, weighted average with the properties of air
VP	Measured according the procedure proposed by Sanchirico et al. (2018) [5]
ΔH_{dev}	DSC analysis (N_2 flow, 20°C/min)
S_l	CHEMKIN calculation [23], once determined the composition of gases produced by devolatilization through TG/FTIR analysis and/or by literature data
T_{ign}	Weight average value computed according to the Le Chatelier rule, once determined the composition of gases produced by devolatilization through TG/FTIR analysis and/or by literature data
ρ_{dev} and $Cp_{gas,II}$	Weight average values of gas density and heat capacity in the II zone computed once determined the composition of gases produced by devolatilization through TG/FTIR analysis and/or by literature data

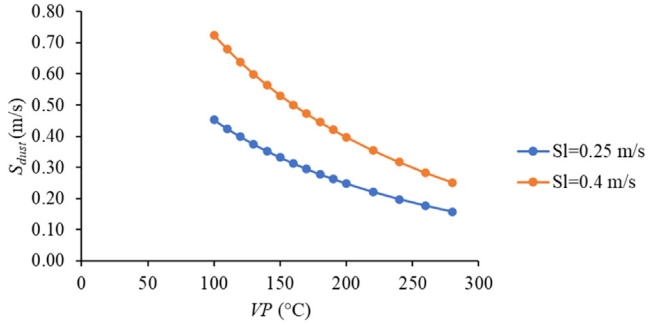

Fig. 4. S_{dust} profiles as functions of VP and parametric in S_l.

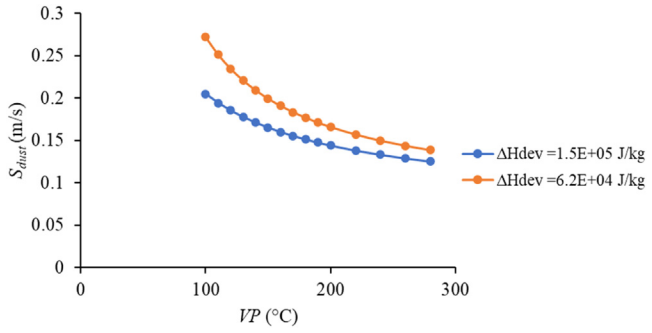

Fig. 5. S_{dust} profiles as functions of VP and parametric in ΔH_{dev}.

agation. It is also worth noting that in ΔH_{dev} the effect of dust particles diameter is included.

The theoretical model was applied to calculate the laminar burning velocity of cornstarch-air and lycopodium-air mixtures. To determine the composition of gases produced by devolatilization for each dust, literature data were used for cornstarch. For lycopodium, literature data were not available and *TG/FTIR* analysis was carried out. All the details are described in the following paragraphs.

- *Application of the model to cornstarch dust*

In the case of cornstarch dust, ρ_{dust} and Cp_{dust} were equal to 1500 kg/m^3 and 1970 J/kg°C, respectively [30]. *VP* was measured by following the procedure proposed by Sanchirico et al. (2018) [5] and was found equal to 260±0.5°C. Figure 6 shows the TG/DSC analysis of cornstarch dust carried out with nitrogen atmosphere and β=20°C/min. In particular, the trends of weight loss percentage as well as heat flow are reported as function of temperature from ambient to 1000°C. From this analysis, the volatile content as well as the decomposition heat can be calculated. Volatile content was calculated by using the following equation:

$$VM = W_{\%}\ (1000^{\circ}C) - W_{\%}\ (110\ ^{\circ}C) \quad (2)$$

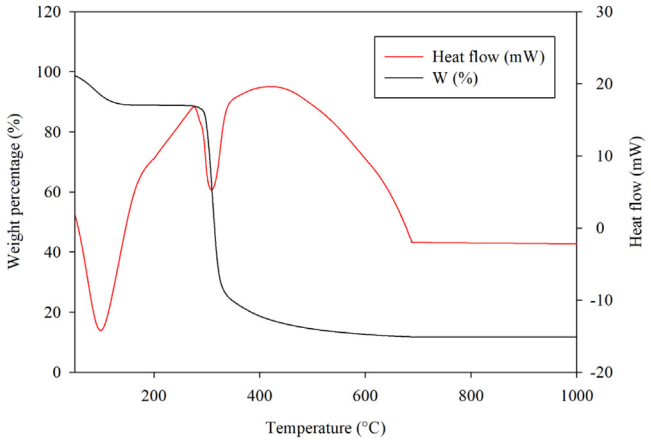

Fig. 6. Weight percentage (black line) and heat flow (red line) as functions of temperature as recorded during TG/DSC analysis, cornstarch dust, N_2 atmosphere, β=20°C/min.

Where $W_{\%}$ $(1000^{\circ}C)$ is the weight percentage at 1000°C at the end of the thermal analysis (≈10%) while $W_{\%}$ $(110\ ^{\circ}C)$ is the weight percentage at 110°C after the moisture loss (≈90%). Volatile matter was determined equal to 80%wt. As regard the heat flow profile, it shows two main peaks: the former relative to water desorption up to 200°C while the latter, characterized by a peak temperature of 310°C, related to cornstarch decomposition. The heat of devolatilization was assessed by manually integrating the heat flow curve in correspondence of the second peak and the value was ΔH_{dev}=1.54E+05 J/kg. It is worth noting that starting from 700°C the heat flow trend was reported as flat only for graphical purposes.

In the case of cornstarch, the compositions of gases produced by devolatilization were taken from literature data, at different temperature. In particular, Mazurkiewicz et al. (1993) reported results of tests carried out by heating to different temperatures (300, 450, 550°C) cornstarch dust, at stoichiometric concentration (233 g/m^3), in a cylindrical steel container located in an oven [14]. In the test vessel, no vacuum conditions were realised. Thus, the composition of the product gases was analysed by means of a gas chromatograph after thermal decomposition of the dust, in the presence of air. The cornstarch used consists of particles nearly spherical in shape with a mass mean diameter of 15 µm. The results of measurement of the gas composition showed that, at a temperature of 300°C the reactions of decomposition of dust produces mainly CO_2 and a small amount of CO. At higher temperatures, the relation between CO and CO_2 becomes inverse, some methane and hydrogen occurring in addition. In our calculations, we tested the pyrolysis composition obtained by Mazurkiewicz et al. (1993) at 450 and 550°C [14]. All the properties values used for cornstarch are summarized in Table 2 as well as the proce-

Table 2
Theoretical model parameters, procedures and values for cornstarch.

Parameter	Value	Procedure
ρ_{dust} and Cp_{dust}	1500 kg/m^3 and 1970 J/kg°C	Dust properties [30]
VP	260°C	Measured according the procedure proposed by Sanchirico et al. (2018) [5]
ΔH_{dev}	1.54E+05 J/kg	DSC analysis (N_2 flow, 20°C/min)
S_l	Variable	CHEMKIN calculation [23], once determined the composition of gases produced by literature data [14]
T_{ign}	Variable	Weight average value computed according to the Le Chatelier rule, once determined the composition of gases produced by literature data [14]
ρ_{dev} and $Cp_{gas,II}$	Variable	Weight average values of gas density and heat capacity in the II zone computed once determined the composition of gases produced by literature data [14]

Table 3
Volatiles produced by the pyrolysis of cornstarch, oxygen and nitrogen at varying the dust concentration at 450°C. The stoichiometric oxygen amount as well as all the calculated parameters are also shown.

C (g/m^3)	H_2 (%)	O_2 (%)	N_2 (%)	CO (%)	CH_4 (%)	CO_2 (%)	$O_{2,stoich}$ (%)	ρ_{dev} (kg/m^3)	S_l (m/s)	$Cp_{gas,II}$ (J/kg°C)	T_{ign} (°C)	f_{dust} (-)	$\rho_{dust+air}$ (kg/m^3)	$Cp_{dust+air}$ (J/kg°C)
400	0.17	16.84	63.36	8.46	3.62	7.55	11.55	1.30	0.17	1071	586.5	0.00027	1.70	1071
500	0.20	16.05	60.37	10.08	4.31	8.99	13.76	1.31	0.25	1081	586.5	0.00033	1.81	1082
550	0.23	15.33	57.66	11.55	4.94	10.30	15.76	1.31	0.29	1086	586.5	0.00037	1.86	1087
600	0.26	14.67	55.17	12.89	5.51	11.50	17.60	1.31	0.32	1091	586.5	0.00040	1.91	1091
650	0.29	14.06	52.89	14.12	6.04	12.60	19.28	1.31	0.327	1096	586.5	0.00043	1.96	1096
700	0.31	13.50	50.79	15.26	6.52	13.61	20.83	1.31	0.323	1100	586.5	0.00047	2.01	1100

Table 4
Volatiles produced by the pyrolysis of cornstarch, oxygen and nitrogen at varying the dust concentration at 550°C. The stoichiometric oxygen amount as well as all the calculated parameters are also shown.

C (g/m^3)	H_2 (%)	O_2 (%)	N_2 (%)	CO (%)	CH_4 (%)	CO_2 (%)	$O_{2,stoich}$ (%)	ρ_{dev} (kg/m^3)	S_l (m/s)	$Cp_{gas,II}$ (J/kg°C)	T_{ign} (°C)	f_{dust} (-)	$\rho_{dust+air}$ (kg/m^3)	$Cp_{dust+air}$ (J/kg°C)
233	0.66	18.12	68.18	5.35	3.43	4.25	9.87	1.28	0.074	1138	580	0.00016	1.51	1138
250	0.70	17.95	67.51	5.68	3.65	4.52	10.48	1.28	0.106	1146	580	0.00017	1.53	1146
270	0.75	17.74	66.73	6.07	3.89	4.82	11.19	1.28	0.140	1155	580	0.00018	1.55	1155
300	0.82	17.44	65.60	6.63	4.25	5.27	12.22	1.28	0.190	1168	580	0.00020	1.58	1168
400	1.03	16.50	62.09	8.36	5.36	6.65	15.43	1.28	0.350	1208	580	0.00027	1.68	1208
428	1.09	16.26	61.17	8.81	5.66	7.01	16.26	1.27	0.367	1218	580	0.00029	1.70	1219
500	1.23	15.67	58.93	9.92	6.36	7.89	18.30	1.27	0.380	1244	580	0.00033	1.77	1244
550	1.31	15.28	57.47	10.64	6.83	8.46	19.63	1.27	0.340	1261	580	0.00037	1.82	1261
600	1.40	14.91	56.09	11.33	7.27	9.01	20.90	1.27	0.260	1276	580	0.00040	1.87	1277

dure involved for their calculations/measurements. As regards the parameters which values are variable (i.e., functions of dust concentration), their calculations were performed once set the composition of gases produced by literature data [14]. In particular, Mazurkiewicz et al. (1993) determined the thermal decomposition products of the cornstarch at two temperatures, 450°C and 550°C. The composition at 300°C was excluded due to the very low laminar burning velocity of produced gases (<0.07 m/s).

In Tables 3 and 4 the composition of volatiles at varying the dust concentration in a closed vessel are reported for the composition at 450°C and 550°C, respectively. Moreover, all the calculated parameters as well as S_{dust} are listed in the above mentioned Tables 3 and 4. In Fig. S1-S12 the temperature, axial velocities and produced gaseous composition as computed by CHEMKIN calculations for cornstarch are reported by the way of example for some dust concentration values. In Fig. 7, the dust laminar burning velocity obtained by the theoretical model calculations are shown starting from the volatile compositions at 450°C and 550°C. Literature data ([11–16]) obtained with different experimental rigs, granulometries and concentration are also reported (literature data were shown and discussed in Fig. 2). From the data shown in Fig. 7, it appears that a very good agreement is obtained with the data provided by Krause and Kasch (1994) [31].

- *Application of the model to lycopodium dust*

In the case of lycopodium dust, ρ_{dust} and Cp_{dust} were equal to 1000 kg/m^3 and 1004.8 J/kg°C, respectively [5]. *VP* was measured by following the procedure proposed by Sanchirico et al. (2018) [5] and was found equal to 210±0.5°C.

As in the case of cornstarch dust, thermal analysis in inert atmosphere was carried out to assess the volatile matter as well as the heat of devolatilization. Figure 8 shows both the weight loss percentage and the heat flow versus the temperature as recorded during the test. Volatile matter was determined equal to 87%wt of the dried sample initial weight by measuring the weight loss (Eq. (7)). Differently from cornstarch, the lycopodium decomposition occurs through several phenomena as can be seen clearly by looking at the high number of peaks in the first derivative of *TG* curve (*DTG*) (Fig. 9). Consequently, the heat of devolatilization was calculated as the sum of all the results coming from the integration of the heat flow curve starting from the onset temperature (200°C). The heat of devolatilization was found equal to 3.07E+05 J/kg.

For lycopodium, literature data relative to volatile composition are not available. Consequently, *TG/FTIR* analysis was carried out. Particularly, the lycopodium sample was heated up to *VP*, that is the lowest temperature at which the mixture produced volatiles-air is flammable, and kept at this temperature for about 30 min. Figure 10 shows both the weight percentage and the temperature as functions of the time as recorded during this test. The outflow was directly sent to an *FTIR* cell analyser through a transfer line to continuously analyse the produced volatiles. It is worth noting that by means of *FTIR*, we had no possibility to assess the composition of produced gases but it was possible to identify the main products. Surprisingly, as shown by the FTIR

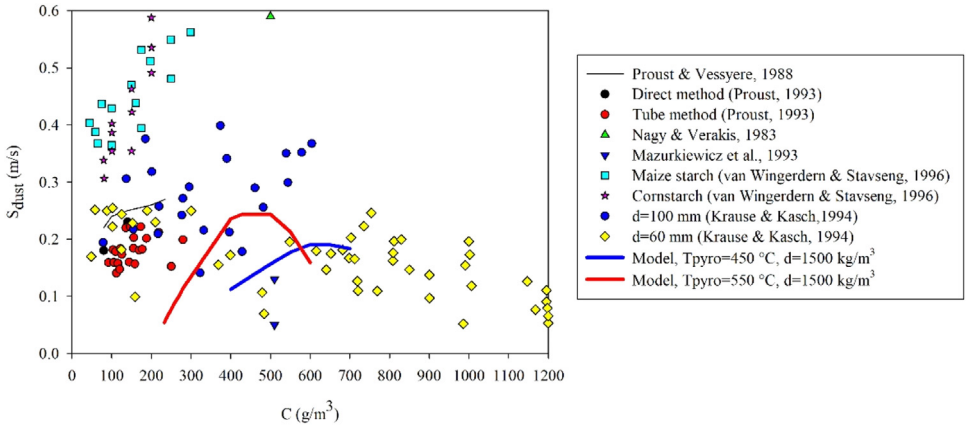

Fig. 7. S_{dust} as function of cornstarch concentration as computed at pyrolysis temperature: 450°C and 550°C. Literature data are also shown ([11–16]).

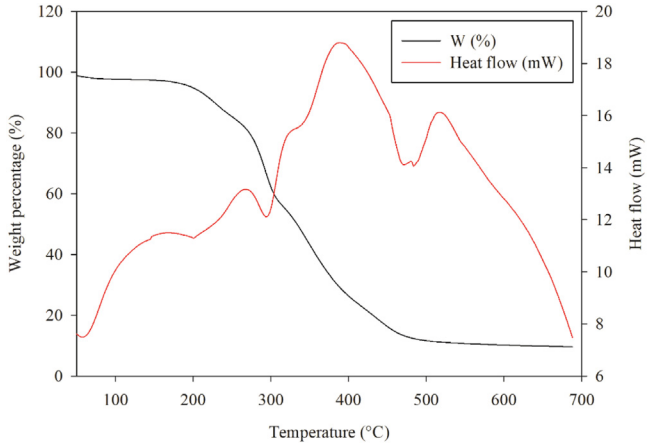

Fig. 8. Weight percentage (black line) and heat flow (red line) as functions of temperature as recorded during TG/DSC analysis, lycopodium dust, N_2 atmosphere, β=20°C/min.

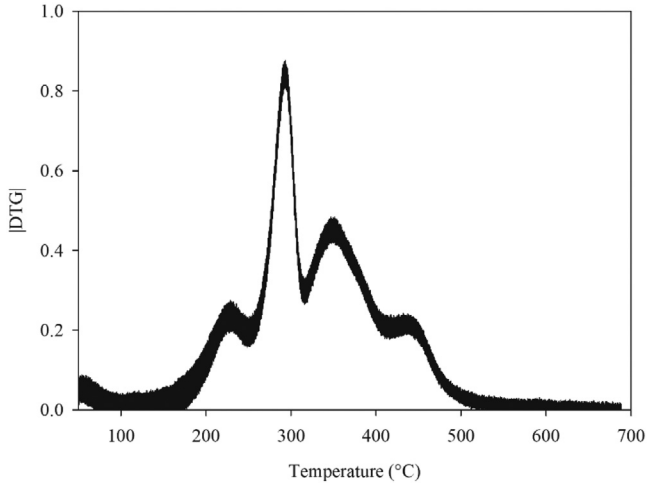

Fig. 9. DTG as functions of temperature as recorded during TG/DSC analysis, lycopodium dust, N_2 atmosphere, β=20°C/min.

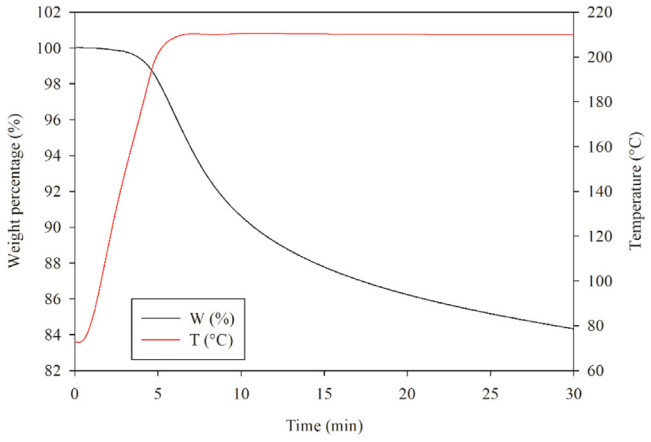

Fig. 10. Weight percentage (black line) and temperature (red line) as functions of time as recorded during TG/DSC analysis, lycopodium dust, airflow.

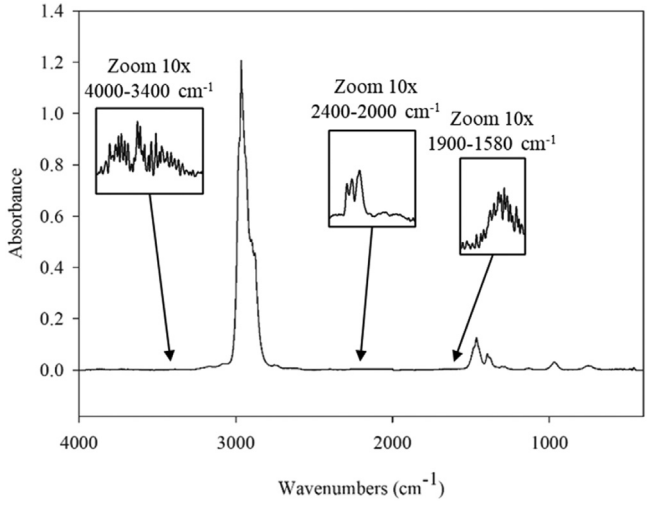

Fig. 11. FTIR spectrum of the gaseous species produced during the test showed in Fig. 10, airflow, T = 210°C, lycopodium dust.

spectrum in Fig. 11, butane was found as the main component of lycopodium [29]. Water (in 4000–3400 cm^{-1} and 1900–1580 cm^{-1} ranges), carbon monoxide and dioxide (in 2400–2000 cm^{-1} range) were found in traces. Consequently, for all the calculations, we considered that the devolatilization of lycopodium leads to the formation of a butane current.

All the properties values used are summarized in Table 5 as well as the procedure involved for their calculations/measurements. As regards the parameters which values

Table 5
Theoretical model parameters, procedures and values for lycopodium.

Parameter	Value	Procedure
ρ_{dust} and Cp_{dust}	1000 kg/m^3 and 1004.8 J/kg°C	Dust properties [5]
VP	210°C	Measured according the procedure proposed by Sanchirico et al. (2018) [5]
ΔH_{dev}	3.07E+05 J/kg	DSC analysis (N_2 flow, 20°C/min)
S_l	Variable	CHEMKIN calculation [23], once determined the composition of gases produced by TG/FTIR analysis
T_{ign}	Variable	Weight average value computed according to the Le Chatelier rule, once determined the composition of gases produced by TG/FTIR analysis
ρ_{dev} and $Cp_{gas,II}$	Variable	Weight average values of gas density and heat capacity in the II zone computed once determined the composition of gases produced by TG/FTIR analysis

Table 6
Volatiles produced by the pyrolysis of lycopodium, oxygen and nitrogen at varying the dust concentration. The stoichiometric oxygen amount as well as all the calculated parameters are also shown.

C (g/m^3)	C_4H_{10} (%)	O_2 (%)	N_2 (%)	$O_{2,stoich}$ (%)	ρ_{dev} (kg/m^3)	S_l (m/s)	$Cp_{gas,II}$ (J/kg°C)	T_{ign} (°C)	f_{dust} (-)	$\rho_{dust+air}$ (kg/m^3)	$Cp_{dust+air}$ (J/kg°C)
40	1.65	20.65	77.69	10.75	1.30	0.08	0.246	405	3.40E-05	1.34	1027
50	2.06	20.57	77.37	13.38	1.31	0.23	0.246	405	4.26E-05	1.36	1030
90	3.65	20.23	76.12	23.70	1.32	0.35	0.249	405	7.66E-05	1.41	1041
100	4.03	20.15	75.81	26.23	1.32	0.26	0.250	405	8.51E-05	1.42	1044
150	5.93	19.75	74.31	38.56	1.34	0.07	0.253	405	1.28E-04	1.49	1057
200	7.76	19.37	72.87	50.42	1.36	0.05	0.256	405	1.70E-04	1.56	1070
250	9.51	19.00	71.49	61.82	1.37	0.04	0.259	405	2.13E-04	1.62	1083

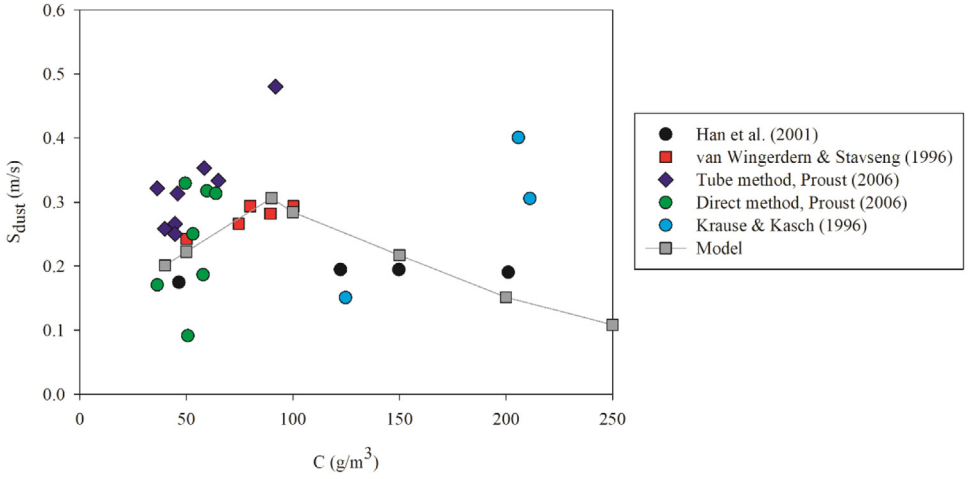

Fig. 12. S_{dust} as function of lycopodium concentration as computed at pyrolysis temperature: 450°C and 550°C. Literature data are also shown ([11–16]).

are variable (i.e., functions of dust concentration), their calculations were performed once determined the composition of gases produced by TG/FTIR analysis [14]. In Table 6 the compositions of volatiles at varying the dust concentration in a closed vessel are reported. Moreover, all the calculated parameters as well as S_{dust} are listed in Table 6. In **Fig. S13–16** the temperature, axial velocities and produced gaseous composition as computed by CHEMKIN calculations for lycopodium are reported by the way of example for some dust concentration values.

In Fig. 12, the dust laminar burning velocity obtained by the theoretical model calculations are shown starting from the volatile compositions reported in Table 6. Literature data obtained with different experimental rigs, granulometries and concentration are also reported ([11,12,15,16,32]). Han et al. (2001) studied the flame propagation mechanisms in lycopodium dust clouds within a vertical duct of 1800 mm height with 150 mm × 150 mm square cross-section where the dust dispersion was realized though the elutriation above a fluidized bed for lycopodium-air (mean particle diameter 31 µm, concentration 30–100 g/m^3) [32]. Proust (2006) assessed the lycopodium S_l (i.e., S_{dust}) within a 1.5 m long tube where the dust dispersion was realized though the elutriation above a fluidized bed for lycopodium-air (mean particle diameter 31 µm, concentration 30–100 g/m^3) through the tube and direct methods [33]. van Wingerden and Stavseng (1996) measured the laminar burning velocity of the lycopodium-air flame (mean particle diameter 30 µm, concentration 50–175 g/m^3) in an 1.6 m long vertical tube made of transparent polycarbonate where the dust was supplied continuously into the top of the tube from a horizontally vibrating sieve and a vibratory dust feeder [15]. The burning velocity in laminar flows was studied in a vertical cylindrical tube of 2 m in length and 300 mm in diameter where dust was layered on a porous filter plate and elutriated in a fluidized bed at the beginning of each experiment by Krause and Kasch (1994) (mean particle diameter 30 µm, concentration 100–600 g/m^3) [16]. From the experimental and model data shown in Fig. 12, it appears that the model is quite in agreement for low concentrations, even if as in the case of cornstarch, there is a large scattering of the experimental data due to the different experimental conditions.

5. Discussion about the effects of the initial pressure and temperature

In this work, the effect of the initial pressure and temperature was not taken into account. However, by combining the expression found for S_{dust} (Eq. (6)) with the Eq. (4.51) of [1], a useful equation can be found as reported in the following:

$$S_{dust,T,P} = S_{dust}\left(\frac{T_{unburned}}{T_{amb}}\right)^{2}\left(\frac{P_{amb}}{P_{unburned}}\right)^{\beta} \quad (8)$$

Where $S_{dust,T,P}$ (m/s) is the theoretical burning velocity of a combustible dust as a function of the initial temperature and pressure, T_{amb} (°C) is set at 25°C as reported in Eq. (6), P_{amb} (bar) is set at 1 bar, $T_{unburned}$ (°C) is the temperature of unburned dust, $P_{unburned}$ (bar) is the pressure at which ignition occurs, β (-) is an empirical constant. The verification of this relationship will be performed in a future work, eventually also using the β parameter as an adjustable parameter.

6. Discussion about the effects of flame curvature and flame stretch

In the theoretical model presented in this paper, the calculated flame propagation rate is considered as unstretched. For the validation of the model, the limited data available for the examined and presented as application examples dusts were used. Generally, the experimental data collected came from tests conducted in tubular set-ups and through the application of tube methods or direct methods.

In general, the assessment of flame propagation velocity in these works is conducted sufficiently far from the point of ignition where the flame is predominantly spherical, through optical methods or by using thermocouples as probes. No evaluation of the stretch is generally present in the collected literature works, with the exception of the work by Proust (2006) [33]. In this work, the flame propagation velocity of cornstarch and lycopodium is evaluated in a tube with a square cross-section and, for cornstarch only, the evaluation is conducted in tubes of different cross-sectional dimensions. Results, reported in Fig. 17 of [33], showed that due to different levels of flame stretching, that is a function of 1/D with D (m) the set-up diameter, the variation in laminar flame speed can achieve also ± 30%. For this reason, in addition to turbulence effect, also uncontrolled stretching of the flame may explain the scattering of the results as also summarized and reported in Fig. 13.

7. Potential of the model

The mathematical model here developed is characterized by both potential and limitations (as reported in Section 3).

To overcome these limitations, the mathematical model will be extended for the purpose of considering radiative phenomena. Moreover, an *ad-hoc* measurements must be carried out to assess volatiles amount and composition at different heating rates and dust concentration.

However, there are some fundamental potentials such as:

- It is a simple model, based on some preliminary material characterization experiments, to obtain an order of magnitude of the laminar velocity. In particular, as shown in Fig. 13, the model is in good agreement with the experimental data in the typical values range of laminar burning velocity while some experimental points scatter, probably due to a scarce control of turbulence and/or concentration (>0.5 m/s).

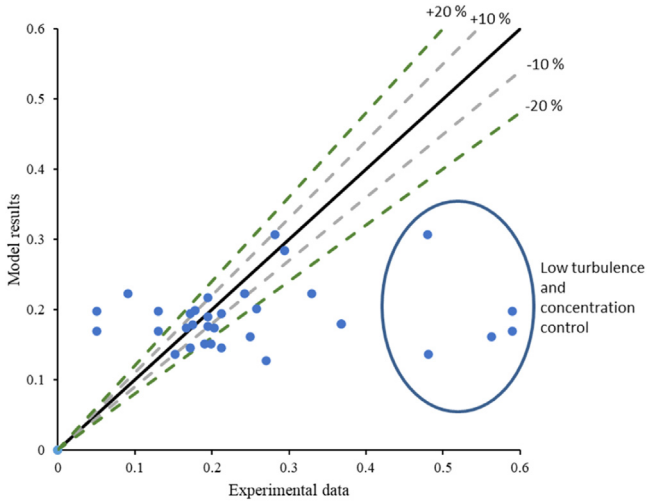

Fig. 13. Parity diagram of model results versus the available experimental data for cornstarch and lycopodium. This diagram is computed for couples of model-experimental data at the same nominal concentration level.

- The approach is based on small scale measurements (samples of a few milligrams) with undispersed powder. This is a key aspect since, as seen in the Introduction section, the key issue of the experimental evaluation of the flame propagation burning velocity lies in the difficulty of uniformly dispersing the dust at a controlled level of turbulence.
- The model can be used to facilitate computational assessments of dust explosions, such as the one carried out by Islas Montero et al. [34]. Firstly, the authors developed a CFD model of a biomass explosion through the computation of the dust dispersion phase and subsequently, they proceeded with the resolution of a system of mass, momentum, energy, species transport, radiation, gas phase combustion, devolatilization equations that is very complex to implement and solve. Through the theoretical model developed here, it would be possible to use the expression obtained for S_{dust} to study the flame propagation of combustible dust as a premixed combustion and using the Peters model to take into account the effect of turbulence [35].

8. Conclusions

The preliminary results of the application of the Mallard-Le Chatelier-inspired theoretical dust flame propagation model were shown. It is worth noting that the way the flame propagates (represented by the laminar burning velocity S_{dust}) depends on several parameters that take into account the thermal behavior of the dust subjected to heating starting from the flame front to the colder layers. As a consequence, a thermal as well as a chemico physical screening of any combustible dust seems to be of crucial importance in order to fully understand the explosive behavior both in terms of intrinsic (laminar) burning velocity but also in terms of flammability/explosibility parameters. Moreover, the analysis of the thermal behavior of combustible dusts can be useful to explain a series of synergistic effects that arise in dust mixtures that can sometimes be more dangerous than pure dusts, as found by Sanchirico et al. (2018) [5].

Declaration of Competing Interest

The authors declare that they have no known competing financial interests or personal relationships that could have appeared to influence the work reported in this paper.

Supplementary materials

Supplementary material associated with this article can be found, in the online version, at doi:10.1016/j.combustflame.2023.112737.

References

[1] R.K. Eckhoff, Dust Explosions in the Process Industries-3rd Edition, Gulf Professional Publishing, 2003.
[2] R.A. Ogle, Dust explosion dynamics, 2016. doi:10.1016/c2014-0-03833-6.
[3] S. Goroshin, J. Palečka, J.M. Bergthorson, Some fundamental aspects of laminar flames in nonvolatile solid fuel suspensions, Prog. Energy Combust. Sci. (2022) 91, doi:10.1016/j.pecs.2022.100994.
[4] M. Portarapillo, G. Luciani, R. Sanchirico, A. Di Benedetto, Ignition mechanism of flammable dust and dust mixtures: an insight through thermogravimetric/differential scanning calorimetry analysis, AIChE J. 66 (2020), doi:10.1002/aic.16256.
[5] R. Sanchirico, V. Di Sarli, A. Di Benedetto, Volatile point of dust mixtures and hybrid mixtures, J. Loss Prev. Process Ind. 56 (2018) 370–377, doi:10.1016/j.jlp.2018.09.014.
[6] A. Di Benedetto, P. Russo, Thermo-kinetic modelling of dust explosions, J. Loss Prev. Process Ind. 20 (2007) 303–309, doi:10.1016/j.jlp.2007.04.001.
[7] A. Di Benedetto, P. Russo, P. Amyotte, N. Marchand, Modelling the effect of particle size on dust explosions, Chem. Eng. Sci. 65 (2010) 772–779, doi:10.1016/j.ces.2009.09.029.
[8] C. Proust, Experimental determination of the maximum flame temperatures and of the laminar burning velocities for some combustible dust-air mixtures, (2014).
[9] W. Gao, T. Mogi, J. Yu, X. Yan, J. Sun, R. Dobashi, Flame propagation mechanisms in dust explosions, J. Loss Prev. Process Ind. 36 (2015) 186–194, doi:10.1016/j.jlp.2014.12.021.
[10] A. Di Benedetto, A. Garcia-Agreda, O. Dufaud, I. Khalili, R. Sanchirico, N. Cuervo, L. Perrin, P. Russo, Flame Propagation of Dust and Gas-Air Mixtures in a Tube, 1, Chia Laguna, Cagliari, Sardinia (2011), pp. 11–13.
[11] C. Proust, B. Veyssiere, Fundamental properties of flames propagating in starch dust-air mixtures, Combust. Sci. Technol. 62 (1988) 149–172, doi:10.1080/00102208808924007.
[12] C. Proust, Experimental determination of the maximum flame temperatures and of the laminar burning velocities for some combustible dust-air mixtures, Int. Colloq. Dust Explos. (1993).
[13] J. Nagy, H.C. Verakis, Development and control of dust explosions, 1983.
[14] J. Mazurkiewicz, J. Jarosinski, P. Wolanski, Investigations of burning properties of cornstarch dust-air flame, Arch. Combust. 13 (1993).
[15] K. Van Wingerden, L. Stavseng, Measurements of the laminar burning velocities in dust-air mixtures, VDI Berichte (1996) 553–564.
[16] U. Krause, T. Kasch, Investigations on Burning Velocities of Dust/Air Mixtures in Laminar Flows, Oral Present., 1994.
[17] H.M. Cassel, A.K. Das Gupta, S. Guruswamy, Factors affecting flame propagation through dust clouds, Symp. Combust. Flame Explos. Phenom. 3 (1948) 185–190, doi:10.1016/S1062-2896(49)80024-9.
[18] R.A. Ogle, J.K. Beddow, A.F. Vetter, L.D. Chen, A thermal theory of laminar premixed dust flame propagation, Combust. Flame 58 (1984) 77–79, doi:10.1016/0010-2180(84)90081-6.
[19] D.R. Ballal, Flame propagation through dust clouds of carbon, coal, aluminum and magnesium in an environment of zero gravity, Proc. R. Soc. London A 385 (1983) 21–51 https://www.scopus.com/inward/record.uri?eid=2-s2.0-0001898866&partnerID&40&md5&b6a68c06a297c9e678ae698f9842c4a2.
[20] I. Glassman, R.A. Yetter, Combustion-Fourth Edition, Elsevier, 2008.
[21] ASTM E502-07, Standard Test Method for Selection and Use of ASTM Standards for the Determination of Flash Point of Chemicals by Closed Cup Methods, ASTM Int, West Conshohocken, PA (1984), pp. 1–6, doi:10.1520/E0502-07E01.priate.
[22] C. Di Blasi, Transition between regimes in the degradation of thermoplastic polymers, Polym. Degrad. Stab. 64 (1999) 359–367, doi:10.1016/S0141-3910(98)00134-7.
[23] AnsysChemkin Theory Manual 17.0, Chemkin® Softw, 2016.
[24] S. Davidson, M. Perkin, An investigation of density determination methods for porous materials, small samples and particulates, Meas. J. Int. Meas. Confed. 46 (2013) 1766–1770, doi:10.1016/j.measurement.2012.11.030.
[25] ASTM D7582-15Standard Test Methods for Proximate Analysis of Coal and Coke by Macro Thermogravimetric Analysis, ASTM Int., West Conshohocken, PA, 2009.
[26] Reaction design: San Diego CHEMKIN-PRO Release, 2019.
[27] G.P. Smith, D.M. Golden, M. Frenklach, N.W. Moriarty, B. Eiteneer, M. Goldenberg, T. Bowman, R.K. Hanson, S. Song, W.J.C. Gardiner, V.V. Lissianski, Z. Qin, GRI-MECH 3.0, 2022 http://www.me.berkeley.edu/gri_mech/.
[28] S.M. Kumaran, D. Shanmugasundaram, K. Narayanaswamy, V. Raghavan, Reduced mechanism for flames of propane, n-butane, and their mixtures for application to burners: development and validation, Int. J. Chem. Kinet. 53 (2021) 731–750, doi:10.1002/kin.21477.
[29] Thermo Scientific™HR Nicolet TGA Vapor Phase library, 2022.
[30] S. Pérez, E. Bertoft, The molecular structures of starch components and their contribution to the architecture of starch granules: a comprehensive review, Starch/Staerke 62 (2010) 389–420, doi:10.1002/star.201000013.
[31] U. Krause, T. Kasch, The influence of flow and turbulence on flame propagation through dust-air mixtures, J. Loss Prev. Process Ind. 13 (2000) 291–298, doi:10.1016/S0950-4230(99)00062-5.
[32] O.-S. Han, M. Yashima, T. Matsuda, H. Matsui, A. Miyake, T. Ogawa, A study of flame propagation mechanisms in lycopodium dust clouds based on dust particles' behavior, J. Loss Prev. Process Ind. 14 (2001) 153–160, doi:10.1016/S0950-4230(00)00049-8.
[33] C. Proust, Flame propagation and combustion in some dust-air mixtures, J. Loss Prev. Process Ind. 19 (2006) 89–100, doi:10.1016/J.JLP.2005.06.026.
[34] A. Islas, A.R. Fernández, C. Betegón, E. Martínez-Pañeda, A. Pandal, Computational assessment of biomass d$\delta\delta$ust explosions in the 20L sphere, Process Saf. Environ. Prot. 165 (2022) 791–814, doi:10.1016/j.psep.2022.07.029.
[35] ANSYS Inc.ANSYS Fluent User's Guide, (2020), 2020.
[36] L. Centrella, M. Portarapillo, G. Luciani, R. Sanchirico, A. Di Benedetto, Synergistic behavior of flammable dust mixtures: A novel classification, J. Hazard. Mater. 397 (2020) 122784, doi:10.1016/j.jhazmat.2020.122784.